of the Barren Island indicates large feeder systems such as the parasitic cones and continuous supply of lava from these parasitic cones below the sea during the recent eruptions. Furthermore, the abrupt fall on the eastern side of the IB is explained by the presence of WAF. A newly identified submarine mount, south of the BI, is associated with the volcanic arc in the Andaman Sea. In addition, the close relationship of the newly identified submarine volcanic mount and BIV is established, because of its proximity to the parasitic cones. Hence, the parasitic cones on the southwestern and southern submarine slopes and the submarine volcanic mounts are developed in association with the recent eruptions in 2005 and 2009. Unlike BIV island, other associated morphotectonic elements in the present study area, viz. IB and Alcock seamount are flat-topped. Furthermore, the slopes facing the Barren Island are characterized by submarine slides, which are completely absent on the other slopes. Although detailed studies are required to constrain the reasons for explaining the presence of submarine slides, it is possible that they may be related to the recent eruptions.

The present study revealed the changes in the configuration of the base of BIV. Effects of recent flows on BIV under the sea are deciphered in the form of thick flows along the western and southwestern slope, extending even up to the base of IB. Furthermore, development of parasitic cones and a newly identified submarine volcanic mount in the present study area also indicate the submarine volcanic activities associated with BIV. Development of numerous feeding sites as expressed in the form of parasitic cones provided huge volume of lava, which in turn pushed the flows to the base of IB. These recent flows reduce the steepness of BIV in the western slopes. This implies that the morphology of the Barren volcanic base is largely modified by the recent eruptions. Furthermore, it is also noteworthy that other morphotectonic elements surrounding the Barren Volcano, viz. Alcock seamount and IB are flat-topped, stable features unlike the BIV.

1. Curray, J. R., Moore, D. G., Lawyer, I. A., Emmel, F. J., Rain, R. W. and Kiecklefer, R., Geological and geophysical investigations of continental margin. *AAPG Mem.*, 1979, **29**, 189–198.
2. Curray, J. R., Tectonics and history of the Andaman Sea region. *J. Asian Earth Sci.*, 2005, **25**, 187–232.
3. Pal, T. *et al.*, The 2005–2006 eruption of the Barren Volcano, Andaman Sea: evolution of basaltic magmatism in island arc setting of Andaman–Java subduction complex. *J. Asian Earth Sci.*, 2010, **39**, 12–23.
4. Roy, T. K. and Chopra, N. N., Wrench faulting in Andaman forearc basin, India. In Proceedings Offshore Technology Conference, Houston, Texas, 1987, vol. 19, pp. 393–404.
5. Curray, J. R., Geological history of the Bengal geosyncline. *J. Assoc. Expl. Geophys*., 1991, **XII**, 209–219.
6. Ware, C. *et al.*, A system for cleaning high volume bathymetry. *Int. Hydrogr. Rev.*, 1992, **XIX**(2), 77–94.
7. Awasthi, N. *et al.*, Major ash eruptions of Barren Island volcano (Andaman Sea) during the past 72 Kyr: clues from a sediment core record. *Bull. Volcanol*., 2010, **72**, 1131–1136.
8. Sheth, H. C., Ray, J. S., Bhutani, R., Kumar, A. and Awasthi, N., The latest (2008–09) eruption of Barren Island volcano, and some thoughts on its hazards, logistics and geotourism aspects. *Curr. Sci.*, 2010, **98**, 620–626.
9. Sheth, H. C., Ray, J. S., Kumar, A., Bhutani, R. and Awasthi, N., Toothpaste lava from the Barren Island volcano (Andaman Sea). *J. Volcanol. Geotherm. Res.*, 2011, **202**, 73–82.
10. Luhr, J. F. and Haldar, D., Barren Island volcano (NE Indian Ocean): island-arc high alumina basalts produced by troctolite contamination. *J. Volcanol. Geotherm. Res*., 2006, **149**, 177–212.
11. Sheth, H. C., Ray, J. S., Bhutani, R., Kumar, A. and Smitha, R. S., Volcanology and eruptive styles of Barren Island: an active mafic stratovolcano in the Andaman Sea, NE Indian Ocean. *Bull. Volcanol*., 2009, **71**, 1021–1039.

ACKNOWLEDGEMENTS. We thank our colleagues on the cruise SM-220 and especially the Chief Scientist under whose supervision the cruise was undertaken. We also thank the Deputy Director General, Eastern Region, Geological Survey of India (GSI), Kolkata for financial assistance and the Director General, GSI, Kolkata for permission to publish this work. Processing facility for multibeam data provided by the OPEC-I, M&CSD, GSI, Kolkata is acknowledged.

Received 3 May 2014; revised accepted 27 October 2014

Comparative study of soil profiles developed on metavolcanic (basaltic) rocks in two different watersheds of Garhwal Himalaya

S. Vyshnavi[1], R. Islam[1,*] and Y. P. Sundriyal[2]

[1]Wadia Institute of Himalayan Geology, Dehradun 248 001, India
[2]H.N.B. Garhwal University (Srinagar), Srinagar 246 174, India

Soil profiles are rarely preserved in the Himalaya due to active tectonics and erosion. We have studied two rarely well-preserved soil profiles developed on metavolcanic rocks namely Alaknanda soil profile (ASP) and Bhilangna soil profile (BSP) in Alaknanda and Bhilangna watersheds of the Garhwal Himalaya. Geochemical studies were carried out to understand the elemental mobility with reference to the least altered rock (LAR) in both the profiles and are compared. Differences in major element behaviour noticed are depletion of Ca and K in ASP, and depletion of Ca and Na in BSP. Trace elements also show variable mobility such as leaching of Rb, U and enrichment of Sr, Ni in ASP. In BSP, behaviour of these elements is just the opposite. Accumulation of ∑REEs in saprolitic layer and depletion in regolith of ASP suggest that rare earth element (REE) mobility took place during advanced stages of weathering. In BSP, increase in REE content from LAR to regolith suggests

*For correspondence. (e-mail: rislam@wihg.res.in)

dominance of chemical weathering over physical weathering. This is also reflected in chemical index of alteration values which suggest variation of climatic parameters such as rainfall in the region.

Keywords: Climate–tectonic interaction, geochemical behaviour, Lesser Himalaya, physical and chemical alterations, weathering.

WEATHERING is irreversible alteration affected by a combination of physical, chemical and biological processes. Weathering processes operate in an open system with complex set of reactions where removal of labile elements and enrichment of immobile elements take place in varied combinations. Studies on weathering are important because many geological processes such as CO_2 consumption, release of nutrients to the ecosystem, development of residual deposits of many metallic and industrial mineral deposits as well as precious and semiprecious minerals, changes in landscape and so on are related to them. In weathering processes, the stability of minerals follow the Goldich stability series. Basalt is an aphanitic igneous rock which forms in the early stages of magmatic crystallization at high temperatures. Further, it contains higher percentage of ferro-magnesian minerals and is susceptible to chemical alteration[1]. Chemical alteration of basalts is considered as one of the major sinks for atmospheric CO_2 (refs 2 and 3). Chemical weathering of basalts in particular is thought to have much greater effect on global CO_2 budget than would be expected from the global extent of basaltic terrains[3–7]. Usually, basalt decomposition is faster (11 times more) than other rock types such as granites under laboratory conditions. They contain more weatherable minerals, which when broken down liberate relatively more nutrient-rich cations than granites and schists[8,9].

Weathering processes lead to the development of soil profile in the advanced stage of chemical alteration[10], which does not retain the pristine composition of the parent rock. Preservation of soil profile depends on the lower rate of erosion and the stability of the landform[11]. In terrains such as the Himalaya, preservation of the soil profile is difficult due to steep slopes and higher rate of erosion. Hence, data on the soil profiles in the Himalayan sector are very limited. Against this backdrop, two soil profiles developed on metavolcanic rocks located in the Alaknanda and Bhilangna valleys of Garhwal Lesser Himalaya have been studied in detail to understand weathering in relation to climate and tectonics. These two soil profiles namely, Alaknanda soil profile (ASP) and Bhilangna soil profile (BSP) are developed in two different watersheds. In this study major, trace and rare earth element (REE) analyses have been carried out on samples collected from these two soil profiles to compare the geochemical differences in the soils developed on similar parent rocks, but in two different watersheds. Such a study would help in understanding the impact of climate and tectonics on the development of soil profiles.

The Himalaya is broadly divided into five lithotectonic zones from south to north, each zone having its distinct physiographic features and geological history. They are Sub-Himalaya, Lesser Himalaya, Higher Himalaya, Tethys Himalaya and Trans Himalaya (Figure 1 *a* and *b*). Major thrust systems are identified between these lithotectonic units and are designated as Main Boundary Thrust (MBT), Main Central Thrust (MCT), South Tibetan Detachment System (STDS) and Indus Tsangpo Suture Zone (ITSZ). Himalayan Frontal Thrust (HFT) is at the foothills and demarcates the boundary between Sub-Himalaya and Indo-Gangetic alluvium. Lesser Himalaya is the oldest lithotectonic zone of the Himalaya. It is divided into Inner Lesser Himalaya and Outer Lesser Himalaya, which are in turn separated by North Almora Thrust (NAT)[12]. Damtha (Precambrian) Group is the oldest and forms the base of the Lesser Himalaya, which is further classified as Chakrata and Rautgara formations. The Rautgara Formation consists predominantly of quartzites with inter bands of shale, slates and metavolcanic rocks. The two soil profiles studied here have developed on the metavolcanic rocks of the Rautgara Formation. The identified soil profile ASP (Figure 1 *b*)[13] is located in Rudraprayag–Khankra road section at (30°15′23.3″N; 78°5′55.7″E) near Srinagar in the Alaknanda watershed. The other soil profile is formed at Raunsal village (30°26′40.4″N; 78°40′25.7″) on the bank of river Bhilangna (Figure 1 *c*)[14,15] which is a tributary of river Bhagirathi. Alaknanda and Bhagirathi rivers meet at Deoprayag to form the mighty Ganga river.

The Alaknanda river originates from twin glaciers of Bhagirath Khark and Satopanth at a height of 3641 m. The river Bhilangana emerges from the Khatling glacier located at an altitude of 4500 m. The Alaknanda flows with a smooth unruffled surface and under gentle winds whereas the Bhagirathi rushes with great force down a steep declivity, rearing and foaming over large boulders scattered over its bed. The Alaknanda is twice as big as Bhagirathi[16]. Landslides and sediment movement as debris flow are frequent.

In Alaknanda river valley, a climatic gradient ranging from 1200 mm/a, at the foothills to ~3000 mm/a near the mountain front of Higher Himalaya is observed and nearly 75% of the rainfall occurs during the monsoon months. The annual maximum temperature recorded at Rudraprayag is 45°C during summer and the minimum temperature is 2.5°C during winter. In Bhagirathi watershed, the average annual rainfall is 1236 mm/a. Most of the rainfall occurs during the monsoon months. The maximum temperature is 35°C during the summer season and minimum temperature is 1.8°C in the winter months.

The metavolocanic rocks of the Rautgara Formation are basalts of the Early Proterozoic age which have been metamorphosed under greenschist facies during Himalayan

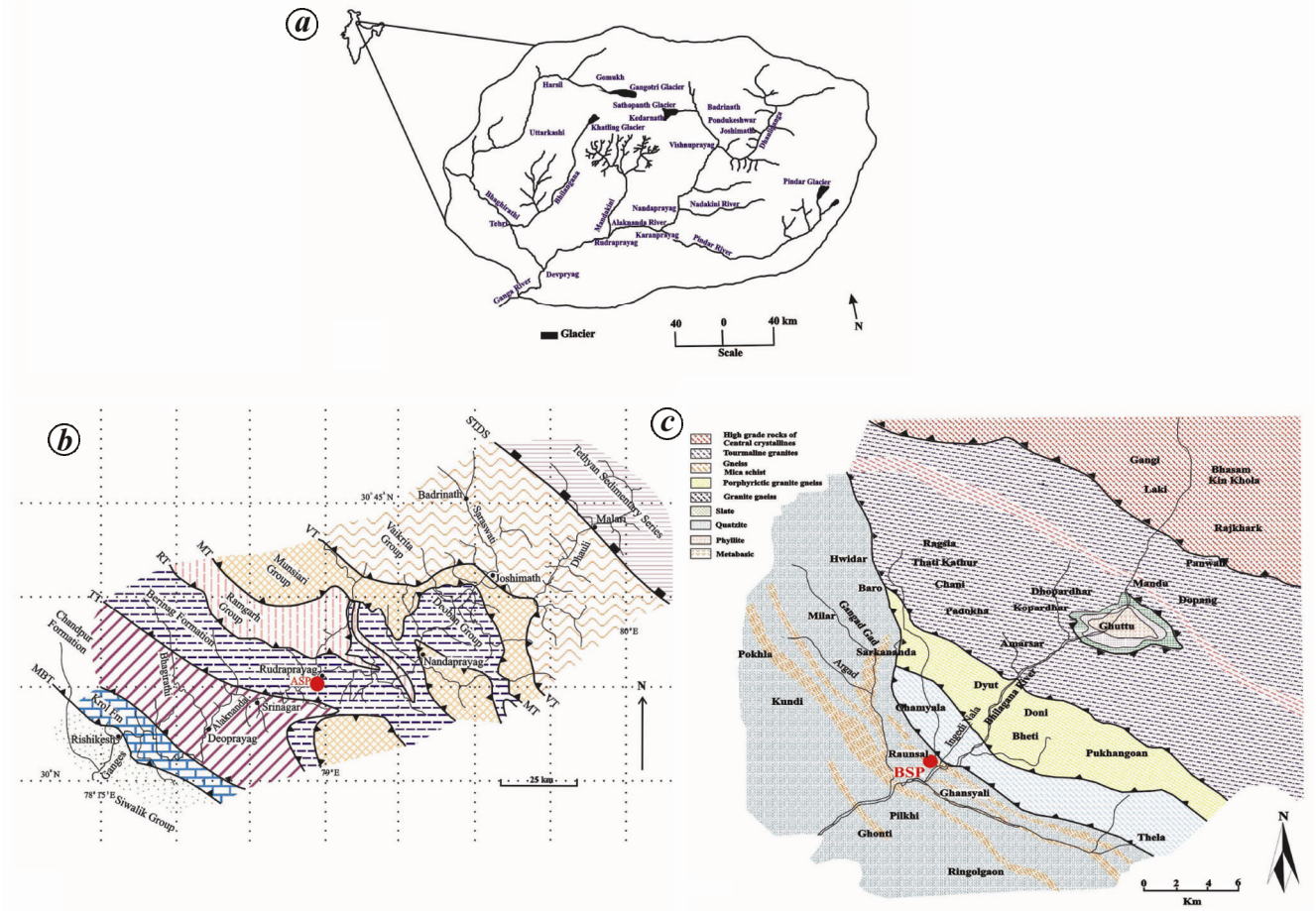

Figure 1. ***a***, Map showing two major river catchments flowing through Garhwal Lesser Himalaya. ***b***, Geological map of Alaknanda river valley in Garhwal Lesser Himalaya, showing the different lithotectonic units of Himalaya (after Ahmad *et al.*[13]). ***c***, Geological map of Bhilangna river valley of Garhwal Lesser Himalaya, showing the different lithotectonic units of Himalaya (after Islam and Thakur[14]; Islam *et al.*[15]). Red dot indicates the location of soil profile.

orogeny. The parent basalts were penecontemporaneously formed during the sedimentation of quartzites[17]. The metavolcanics show relict primary plagioclase and clinopyroxene–augite as dominant minerals. Chlorite, epidote, serpentine, calcite, quartz, biotite, Fe–Ti oxides and sphene occur as accessory minerals. The mafic metavolcanics are prone to chemical alteration due to the presence of high percentage of ferro-magnesian minerals which are more susceptible in the transformation to secondary minerals. Geochemical data reveal that the metavolcanic suit is tholeiitic and are enriched in iron. All the rocks are distinctly enriched in incompatible elements relative to primodial mantle abundances but have distinct continental signature. Chondrite normalized REE data show enriched light REE (LREE) and relatively flat heavy REE (HREE) pattern along with a weak negative Eu anomaly. Enriched large ion lithofile elements (LILE) and distinct negative anomalies for Sr and high field strength elements (HFSE) are observed. These trace and REE characters of metavolcanic rocks of Lesser Himalaya indicate that they originated in a rift related environment and are closely similar to that in rocks of Aravalli and Bundelkhand regions of the Indian shield[17].

Systematic sampling of the two soil profiles was carried out. Colour variation is noticed in the profiles. ASP shows reddish tinge which is due to scraping of ASP profile during dam construction. BSP section is greenish in colour due to the preservation of algal cover that has not been scraped off. Samples were collected from top to bottom after scraping out about 10 cm of the surface to minimize contamination. These profiles are classified into five layers, i.e. least altered rock (LAR) at its base with successive saprock, saprolith, saprolite and regolith overlying it. A total of five samples were collected from each profile and one sample from each layer. Sampling was done as ASP-1 to ASP-5 from ASP (Figure 2 *a*) and BSP-1 to BSP-5 from BSP localities (Figure 2 *b*). The thickness of ASP is 1.48 m and that of BSP is 2.2 m.

Samples were air dried in the laboratory prior to analytics and about 15 g of each sample was powdered to a mesh size of –200 µm in tema mill for geochemical analysis. About 5 g of each of the powdered sample was

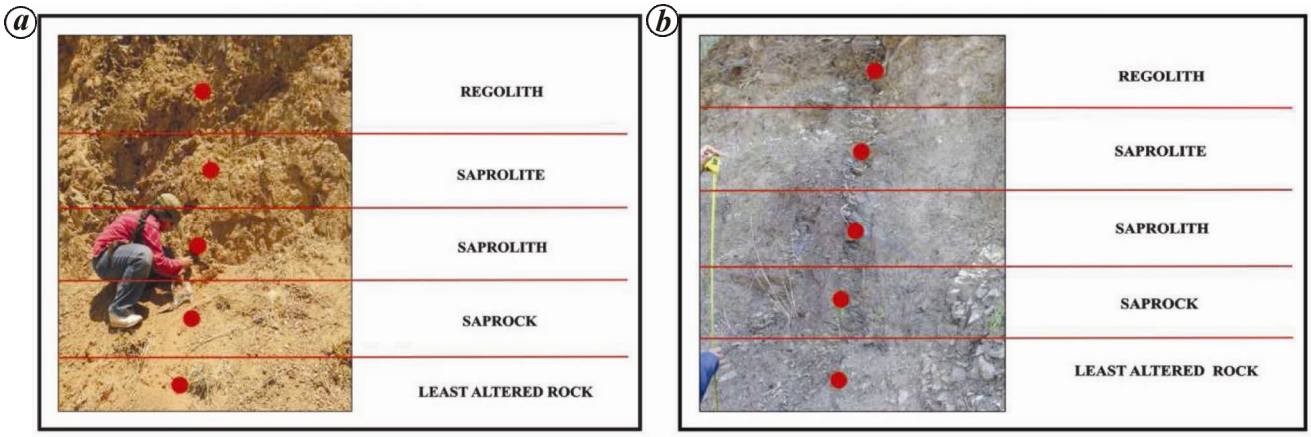

Figure 2. Field photograph of (***a***) ASP metavolcanic soil profile in Alaknanda river valley and (***b***) BSP metavolcanic soil profile in Bhilangna river valley, showing different altered layers. Red dots indicate sample locations.

taken to make pressed pellets using polyvinyl alcohol as binding agent[18,19]. Whole rock analysis was done by X-ray fluorescence (XRF) (Siemens SRS 3000) for major oxides and trace elements. The precision and accuracy were checked using several international reference standards for soils and sediments. The accuracy of measurement is better than 2–5% and precision is <2% (ref. 20). A wet ICP–MS technique (Perkin Elmer) is used for REE analysis using open acid digestion method. Precision for REE is better than 10% (ref. 21). All the analyses were carried out at Wadia Institute of Himalayan Geology, Dehradun.

The data of all the major oxides, trace and REEs of soil profiles (ASP and BSP) are presented in Tables 1 and 2. The 10 major oxides and loss of ignition (LOI) of individual soil profiles are graphically represented in binary plots from least altered rock to regolith. ASP exhibits depletion trend in case of Si, Ca, Mg, Mn, K and P from LAR to regolith, whereas enhancement is noticed in case of Al, Ti, Fe, Na and LOI (Figure 3 *a*). Behaviour of major oxides in BSP shows depletion in Si, Ca, Mg, Na and P, whereas enrichment is noticed in Al, Ti, Fe, Mn, K and LOI relative to least altered rock (Figure 3 *b*). Most of the major oxides show irregular distribution in soil profiles of ASP as well as BSP.

The degree of weathering is calculated using chemical index of alteration (CIA)[22–24].

$$\text{CIA} = \text{Al}_2\text{O}_3/(\text{Al}_2\text{O}_3 + \text{CaO}^* + \text{Na}_2\text{O} + \text{K}_2\text{O}) \times 100 \text{ (molecular proportion)}$$

CaO* is the calcium from silicate rocks only. Ca correction is done to obtain the Ca from the silicate minerals only[25]. The samples of both the profiles are graphically represented in A–CN–K ternary projection using molecular proportion. In ASP section, all the samples plot above the feldspar tie line and form a cluster (Figure 4 *a*). This is attributed to the interaction of tectonic and corresponding climate with rocks leading to alteration, hence the development of *in situ* soil profile. The samples of BSP profile also plot further above the feldspar tie line and lie in the smectite field. Saprock, saprolith, saprolite and regolith are plotted successively above the least altered rock indicating the advancement of weathering. The weathering trend of BSP section is parallel to A–CN tie line and shows continuous alteration with the progression of weathering (Figure 4 *b*). To verify the degree of chemical alteration, we have plotted fresh basalt composition of Early Proterozoic age[26] in the ternary diagrams. The LAR composition of ASP and BSP sections is plotted far away from fresh basalt[26]. Systematic alterations of samples are noticed in successive zones of BSP during the enhancement of weathering and the weathering trend is parallel to A–CN boundary, indicating K leaching in preference to Ca and Na during incipient weathering[27]. However in ASP section, the clustering of samples of all the layers is just above the feldspar tie line and may indicate subdued chemical weathering. This study indicates higher rainfall in the Bhilanagna valley than the Alaknanda valley and successive mineralogical changes due to chemical weathering.

A–CNK–FM plot is used mainly for ferro-magnesian rocks to understand the degree of weathering during advancement of weathering. The samples of ASP section plot above feldspar–FM tie line (Figure 5 *a*) while in BSP section, samples plot further towards the FM apex. This indicates that all the samples of ASP have suffered low to moderate degree of weathering whereas in BSP section, samples indicate moderate to higher degree of alteration with mineralogical changes in saprolith, saprolite and regolith[25]. Samples of both the profiles plot in a single cluster with more affinity towards the FM apex suggesting the depletion of more alkalis and Mg-rich minerals compared to Al; and therefore, the samples plot in between chlorite and smectite fields which indicate the development of Fe–Mg rich clay minerals[27].

Table 1. Geochemical data of ASP soil profile, Alaknanda valley (major oxides are in wt%, trace, rare earth elements are in ppm and total iron as Fe_2O_3). Samples are arranged from least altered rock to regolith

Sample	ASP-5	ASP-4	ASP-3	ASP-2	ASP-1
SiO_2	51.53	51.32	51.7	48.31	48.05
TiO_2	1.05	1.19	1.03	1.32	1.25
Al_2O_3	13.33	13.67	13.74	15.02	15.03
Fe_2O_3	11.69	10.82	9.96	14.42	15.48
MnO	0.22	0.33	0.21	0.15	0.18
MgO	8.13	6.8	7.59	6.56	5.98
CaO	3.72	3.45	3.72	2.52	2.24
Na_2O	2.27	2.68	3.11	2.99	3.63
K_2O	2.43	1.73	1.54	1.37	0.94
P_2O_5	0.14	0.15	0.14	0.15	0.11
LOI	5.75	7.76	5.48	8.97	9.01
Ba	208	210	211	253	260
Cr	139	160	171	141	122
V	251	239	282	274	262
Sc	33	35	32	36	34
Co	54	62	45	52	53
Ni	105	119	112	110	111
Cu	108	151	186	103	171
Zn	133	135	137	148	150
Ga	21	21	18	25	27
Pb	29	14	10	12	13
Th	3	5	3	5	7
Rb	45	39	30	29	18
U	1	1	1	1	1
Sr	105	88	64	187	172
Y	25	29	22	31	26
Zr	135	145	136	174	161
Nb	5	6	5	7	6
La	18.19	18.91	18.93	18.66	15.21
Ce	37.68	40.47	39.30	39.62	30.78
Pr	4.78	5.06	4.97	5.27	4.39
Nd	18.75	19.79	19.25	21.00	17.34
Sm	3.78	4.10	3.96	4.51	3.66
Eu	1.07	1.08	0.75	1.27	0.88
Gd	3.81	4.30	3.83	4.85	3.76
Tb	0.56	0.63	0.57	0.73	0.56
Dy	3.18	3.63	3.21	4.26	3.21
Ho	0.63	0.73	0.61	0.81	0.64
Er	1.63	1.88	1.57	2.02	1.68
Tm	0.24	0.27	0.22	0.29	0.24
Yb	1.48	1.69	1.31	1.72	1.53
Lu	0.21	0.25	0.19	0.25	0.22
CIA	55.96	55.07	52.49	57.76	57.60
CIW	62.90	59.56	56.06	61.26	59.94
PIA	57.65	55.97	52.85	58.76	58.25

Table 2. Geochemical data of BSP soil profile, Bhilangana valley (major oxides are in wt%, trace, rare earth elements are in ppm and total iron as Fe_2O_3). Samples are arranged from least altered rock to regolith

Sample	BSP-5	BSP-4	BSP-3	BSP-2	BSP-1
SiO_2	46.88	45.28	46.65	45.34	44.43
TiO_2	0.82	0.81	0.73	0.82	0.91
Al_2O_3	12.94	13.43	12.94	13.31	14.31
Fe_2O_3	17.3	18.04	20.96	18.64	18.4
MnO	0.17	0.18	0.17	0.18	0.23
MgO	9.62	9.7	9.16	8.55	6.47
CaO	7.32	5.99	5.14	5.35	3.97
Na_2O	1.44	1.59	0.81	0.86	0.75
K_2O	0.83	0.61	0.79	0.88	1.07
P_2O_5	0.13	0.12	0.1	0.11	0.11
LOI	3.26	5.57	7.8	7.35	11.5
Ba	222	226	237	247	257
Cr	224	169	212	215	147
V	158	188	180	197	223
Sc	25	29	31	35	34
Co	61	58	55	54	51
Ni	279	288	286	263	190
Cu	93	85	91	92	100
Zn	100	105	112	107	105
Ga	15	17	16	18	18
Pb	1	2	4	3	5
Th	1	2	1	2	2
Rb	26	20	26	28	39
U	1	1	0	1	1
Sr	189	160	144	174	136
Y	18	19	20	18	21
Zr	94	102	97	100	110
Nb	8	9	8	8	9
La	12.21	14.45	13.8	13.85	16.83
Ce	27.55	32.01	29.13	29.79	39.67
Pr	3.37	4.06	3.86	3.83	4.55
Nd	13.53	16.43	15.72	15.58	18.35
Sm	2.97	3.48	3.38	3.31	3.82
Eu	0.97	1.12	1.01	1.08	1.15
Gd	3.19	3.89	3.67	3.53	4.05
Tb	0.49	0.59	0.57	0.54	0.6
Dy	2.79	3.35	3.2	3.1	3.41
Ho	0.6	0.71	0.69	0.67	0.74
Er	1.58	1.83	1.81	1.74	1.91
Tm	0.24	0.27	0.27	0.26	0.29
Yb	1.58	1.79	1.77	1.71	1.9
Lu	0.24	0.27	0.27	0.25	0.29
CIA	68.73	68.53	77.95	77.20	79.21
CIW	72.18	70.92	82.18	81.71	84.64
PIA	70.71	69.87	81.16	80.58	83.51

The trace elements of ASP and BSP are plotted in binary diagrams. Among the trace elements, Cu, Ni, Zr, Sc, Th and Sr show increase from LAR to regolith, while U, Co and Rb show a decreasing trend in ASP profile. However, the depletion or enhancement of all the trace elements is observed in the saprolithic layer except Cu (Figure 6 *a*). In BSP profile, Cu, U, Zr, Rb, Y, Sc and Th exhibit enrichment in the successive layers relative to LAR. However depletion of Th in saprolith and Cu in saprock is noticed. Transition trace elements such as Ni, Co show continuous depletion throughout the profile (Figure 6 *b*). The zig–zag behaviour may occur due to the repeated depletion and accumulation (development as clay minerals) of the elements in different zones owing to chemical alteration. Cu enrichment occurs due to the breakdown of biotite that leads to the formation of clay minerals. Enrichment of Zr is due to its resistant nature towards weathering processes. Rb behaves similar to K, since these elements reside in potash-bearing hydrous biotite mineral. In general, basalt contains plagioclase

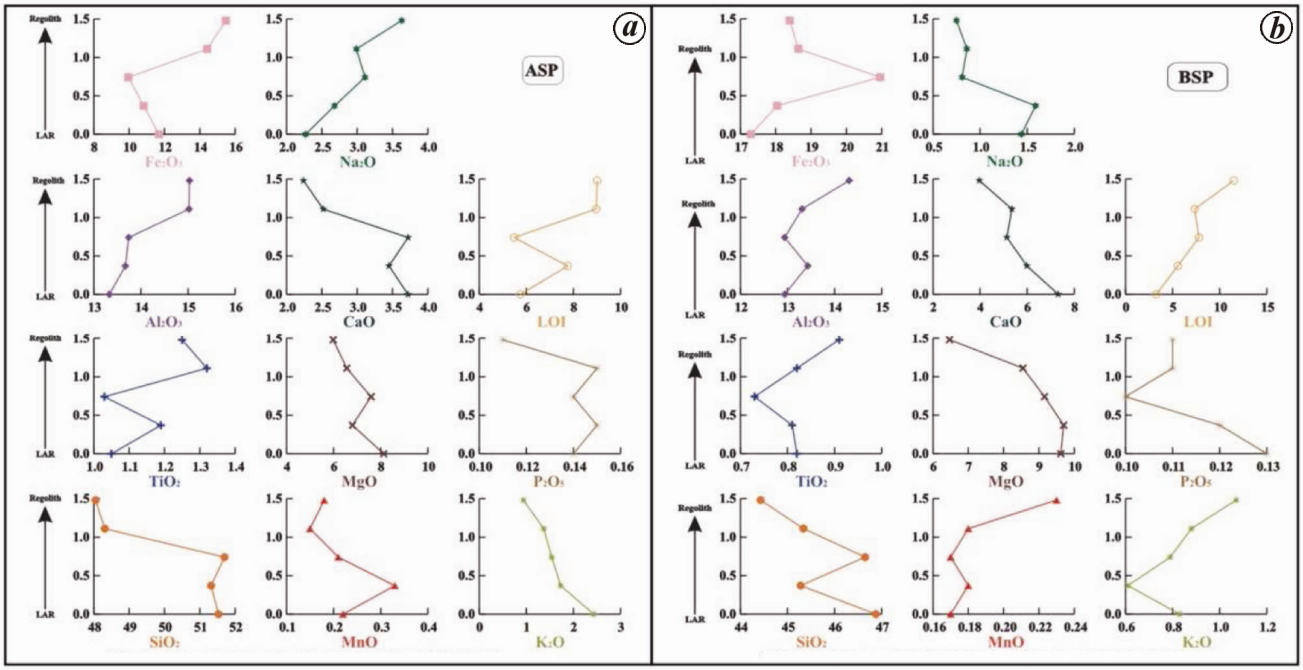

Figure 3. Binary plots of major oxides (in wt%) of (***a***) ASP profile, Alaknanda river valley and (***b***) BSP profile, Bhilangna river valley. LAR represents least altered rock.

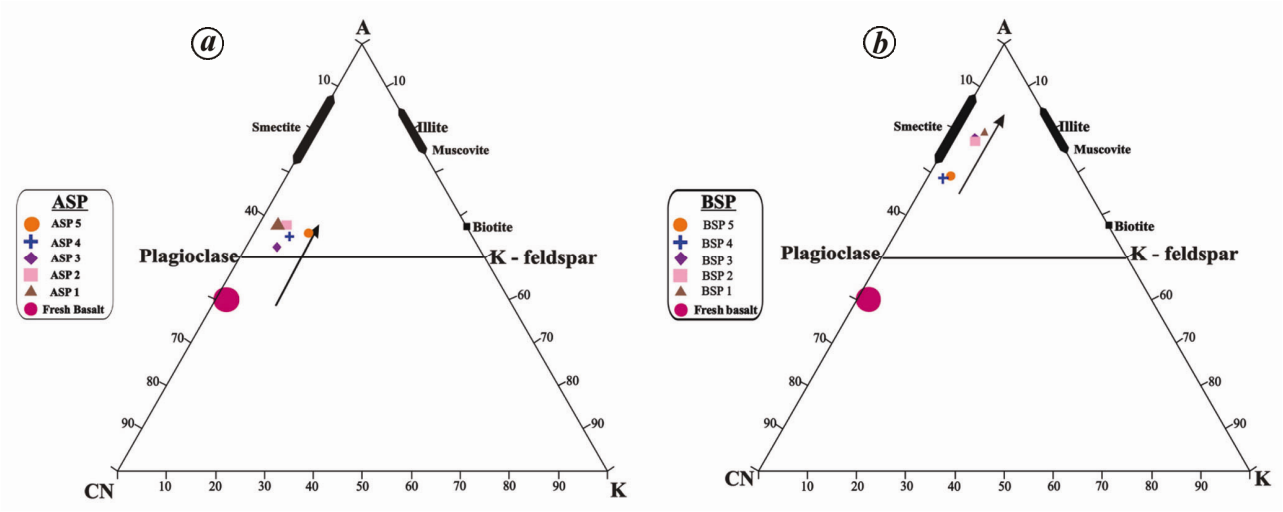

Figure 4. A–CN–K (A = Al_2O_3, CN = CaO* + Na_2O, K = K_2O) ternary plot of (***a***) ASP profile, Alaknanda river valley and (***b***) BSP profile, Bhilangna river valley. Calculated values are in molecular proportion.

which is richer in Ca than Na and; further Sr behaves much similar to Ca. However, in ASP section, Sr shows mismatch with Ca but behaves closely similar to Na. In BSP section, Sr is positively correlated with Ca.

REEs were plotted after normalizing with chondrite value[28] to understand REE mobility during the development of soil profile. Among the REEs, Ce and Eu are the two elements which show different oxidation states. ASP profile shows enriched LREE and depleted HREE pattern with variable negative Eu anomaly through the profile (Figure 7 *a*). However REE concentration (both LREE and HREE) shows depletion in regolith relative to LAR. Presence of negative Eu anomaly throughout the profile suggests breakdown of plagioclase feldspar which leads to the leaching of Eu from the system during the advancement of weathering (Figure 7 *a*); this is also supported by Ca (hosted by calcic plagioclase) leaching[27]. The minor difference between least altered rock and other zones can be related to the absence of major mineralogical changes. BSP profile shows enrichment of all REEs in successive saprock, saprolith, saprolite and regolith with respect to LAR (Figure 7 *b*). Progressive enrichment of REE concentration from LAR to regolith is observed. No significant negative Eu anomaly is observed in the

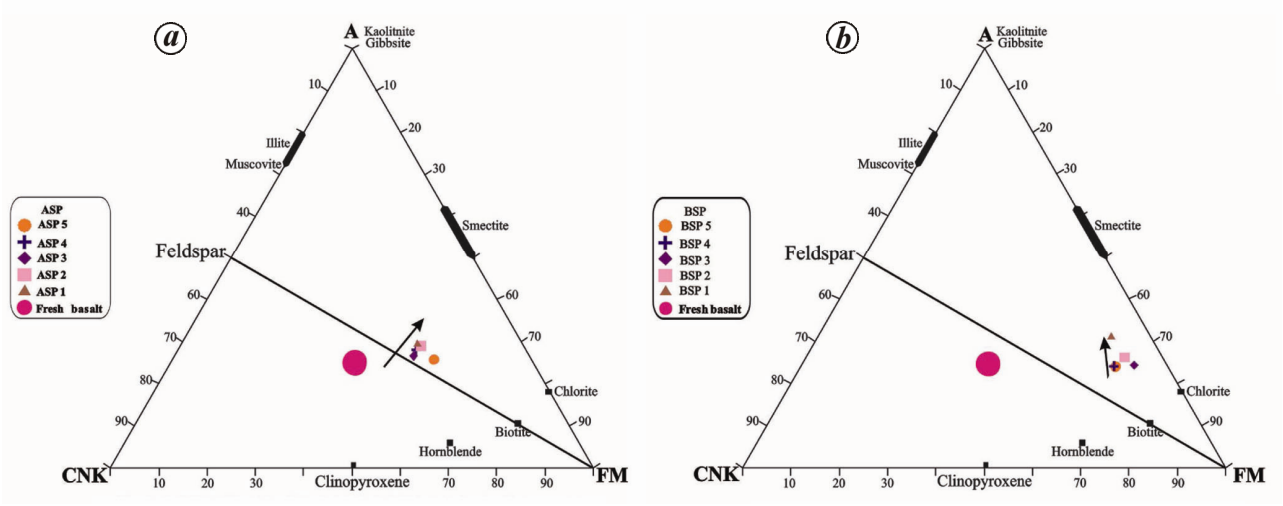

Figure 5. A–CNK–FM (A = Al_2O_3, CNK = CaO* + Na_2O + K_2O, FM = FeO(t) + MgO) ternary plot of (***a***) ASP profile, Alaknanda river valley and (***b***) BSP profile, Bhilangna river valley. Calculated values are in molecular proportion.

saprolithic layer. Negligible Ce anomaly is noticed in both the profiles which further confirm chemical alteration during the advancement of weathering[29].

Garhwal Lesser Himalaya experiences humid subtropical climatic condition which is suitable for the development of soil profile. However, preservation of soil profiles is limited due to fast erosion. Two soil profiles were identified in the Garhwal region of Inner Lesser Himalaya from different watersheds (one from Alaknanda river valley and the other from Bhilangna river valley) and are compared. Both the soil profiles, ASP and BSP show preservation of all the layers, which explains soil persistence due to a rate equal to or greater than that of erosion[11]. ASP profile shows the early stage of calcic-plagioclase and biotite alteration indicated by negative signatures of Ca and K relative to LAR, while Na shows continuous enrichment throughout the profile suggesting retention of sodic plagioclase. However in BSP profile, both Na and Ca are depleted and enrichment of K is noticed. This implies the dissolution of plagioclase[30] and sustainability of K-bearing hydrous biotite mineral because K is more conserved in nature and weathers much slower than Ca and Na[22]. The gradual enrichment of K from LAR to regolith suggests progressive breakdown of plagioclase and is now completely replaced by clay minerals. Generally, Sr mobility is much similar to Ca; and Rb similar to K due to similar valency and ionic radii. However, in case of ASP profile, Sr shows antipathic relationship with Ca, which reveals that enrichment of Ca is due to the precipitation of calcrete[30]. Behaviour of Sr is more or less similar to Na and this shows its association with plagioclase[30]. Drastic depletion of P in BSP compared to ASP profile may suggest more dissolution of apatite in BSP profile and this is due to decrease in pH during precipitation, hence leaching of P[31]. Ni shows significant enrichment in saprock, however depletion of Ni is observed in rest of the profile. In BSP depletion of LILEs indicates the leaching of these elements during progressive alteration; but transition trace elements such as Sc show enrichment due to the development of secondary ferro-magnesian minerals. In A–CN–K ternary plot of ASP profile, all the samples plotted near the feldspar join indicating low to moderate chemical alteration with the advancement of weathering. Further, in A–CNK–FM diagram, samples from all the layers are plotted above feldspar–FM tie line. This confirms that the dissolution of plagioclase and enrichment of ferro-magnesian minerals, hence an affinity towards the FM apex. This affinity may be the indication of the development of secondary ferro-magnesian minerals such as hydrous biotite. BSP profile also shows continuous alteration in the successive layers as observed in an ideal soil profile during progressive weathering. Both A–CN–K and A–CNK–FM ternary diagrams show medium to high range of weathering (CIA: 69–79; CIW: 71–85). The composition of fresh basalt of Early Proterozoic age[26] is plotted in A–CN–K and A–CNK–FM diagrams that reveal that considerable degree of alteration has taken place in LAR of both the profiles; in addition successive chemical change confirms the development of soil profile is *in situ*. Comparison of CIA value between these profiles indicates that ASP has suffered more physical weathering than chemical alteration that is supported by clustering of all the CIA values close to feldspar tie-line in A–CN–K plot. By contrast in BSP section, CIA values progressively increase from LAR to regolith and follow weathering trend parallel to A–CN join, unravels the process of chemical weathering which is dominant over physical weathering in Bhilangna catchment. The value of CIW[32] and PIA[33] indices (where K_2O is eliminated from the equation) also exhibits dissimilar behaviour in both the profiles. Higher value of these parameters in BSP section suggests that alteration of plagioclase and weathering intensity is higher in BSP than ASP. The REE behaviour in these profiles give some

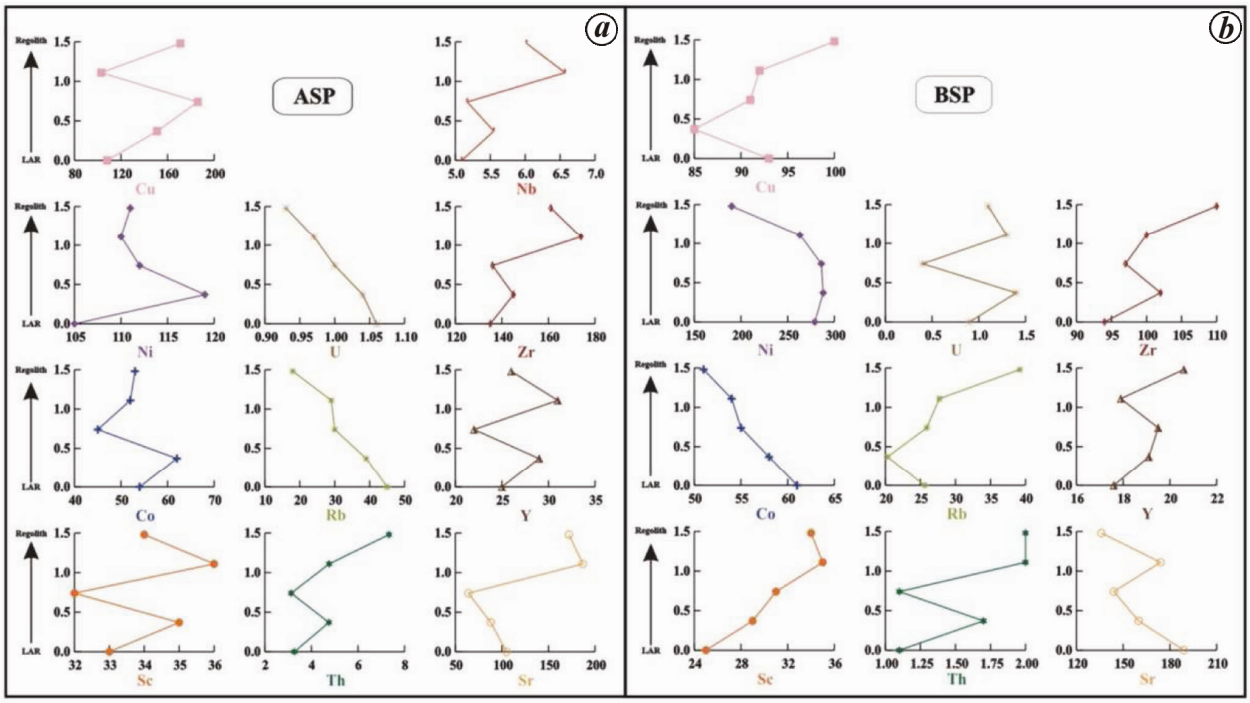

Figure 6. Binary plots of trace elements (in ppm) of (***a***) ASP profile and (***b***) BSP profile showing their elemental distribution from least altered rock to regolith.

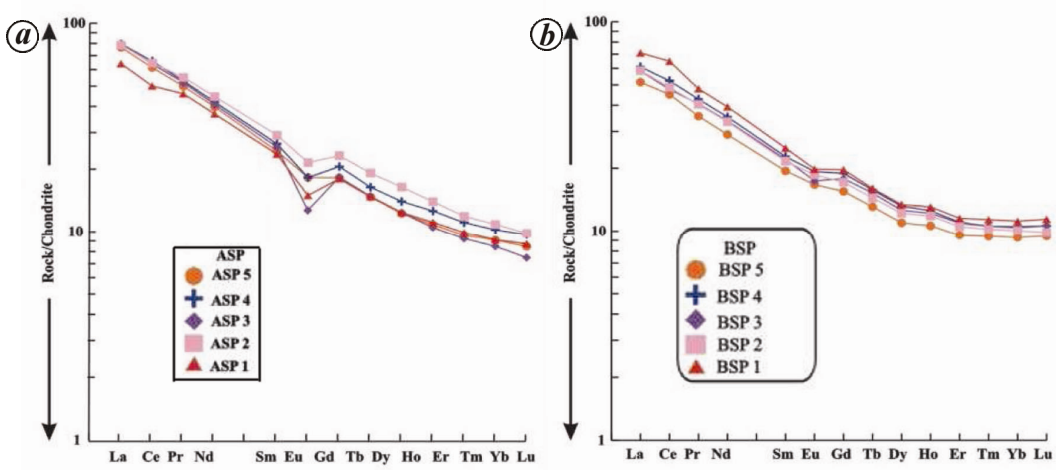

Figure 7. Chondrite normalized REE pattern of (***a***) ASP profile and (***b***) BSP profile developed on metavolcanic rock. Normalized values are after Sun and McDonough[28].

important information about weathering processes. It is generally observed that during chemical weathering, the alteration of minerals control the mobility of REE in the weathering profile. REE plots show enriched LREE and depleted HREE patterns in both the soil profiles, which indicates their accumulation in accessory minerals. Distinct dissimilarity of REEs is observed in both the soil profiles. The distribution of REEs in ASP profile is irregular from LAR to regolith (Figure 7 *a*) and maximum amount of REEs is accumulated in saprolite layer, but drastic depletion is noticed in regolith along with distinct negative Eu anomalies. This may lead to the inference that REE mobility during advanced stages of weathering explains lower/scanty precipitation in Alaknanda valley during the initial stage of the development of soil profile. However in BSP profile, there is an increase in ∑REE content with the progression of weathering from LAR to regolith. This is attributed to continuous increase in ∑REE content in BSP profile of Bhilangna valley due to chemical weathering processes which dominate over physical weathering, corroborating higher rainfall in the region. This hypothesis is also supported by the behaviour of major oxides which is reflected in CIA value.

Therefore, field and geochemical studies in Alaknanda and Bhilangna watersheds of Garhwal Lesser Himalayan region indicate close relationship of weathering with

climate and tectonics. The rocks weather and erode faster in the region where climato-tectonic milieu is more active than stable landform. Further, variations in thickness of soil profiles are noticed due to difference in the erosion rate. Also, tectonic intervention plays a major role in physical weathering process which accelerates the production of different varieties of fractures. These fractures are invaded by rainwater which accelerates the water–rock interaction resulting in the varied degrees of chemical alteration in the soil profiles of Alaknanda river valley. The weathering leads to the development of many secondary minerals as well as raw materials for the growth of vegetation. These secondary minerals are absorbed by the roots and move upward. Based on the above discussion, it is observed that the climate played a major role in altering the rocks and minerals.

Geochemical data lead to the inference that intense and uninterrupted rainfall in Bhilangna river valley as compared to Alaknanda leads to higher degree of leaching/alteration due to the chemical weathering in the former. However in Alaknanda valley, physical weathering played a major role prior to chemical weathering on the development of soil profile in Lesser Himalaya.

1. Goldich, S. S., A study of rock weathering. *J. Geol.*, 1938, **46**, 17–58.
2. Louvat, P. and Allegre, C. J., Present denudation rates at Reunion island determined by river geochemistry: basalt weathering and mass budget between chemical and mechanical erosions. *Geochim. Cosmochim. Acta*, 1997, **61**, 3645–3669.
3. Louvat, P. and Allegre, C. J., Riverine erosion rates on Sao Miguel volcanic island, Azores archipelago. *Chem. Geol.*, 1998, **148**, 177–200.
4. Gíslason, S. R., Arnórsson, S. and Ármannsson, H., Chemical weathering of basalt in southwest Iceland: effects of runoff, age of rocks and vegetative/glacial cover. *Am. J. Sci.*, 1996, **296**, 837–907.
5. Gíslason, S. R., Oelkers, E. H. and Snorrason, A., The role of river suspended material in the global carbon cycle. *Geology*, 2006, **34**, 49–52.
6. Louvat, P., Gíslason, S. R. and Allegre, C. J., Chemical and mechanical erosion rates in Iceland as deduced from river dissolved and solid material. *Am. J. Sci.*, 2008, **308**, 679–726.
7. Gíslason, S. R. *et al.*, Direct evidence of the feedback between climate and weathering. *Earth Planet. Sci. Lett.*, 2009, **277**, 213–222.
8. Pedro, G., La genèse des hydroxydes d'aluminium par altération expérimentale des roches cristallines etle problème des latérites. *Int. Geol. Congress*, 1964, **22**(14), 1–13.
9. Hamdan, J. and Brunham, C. P., The contribution of nutrients from parent material in three deeply weathered soils of Peninsular Malaysia. *Geoderma*, 1996, **74**(3–4), 219–233.
10. Nesbitt, H. W., Mobility and fractionation of rare earth elements during weathering of a granodiorite. *Nature*, 1979, **279**, 206–210.
11. Heimsath, A. M., Dietrich, W. E., Nishiizumi, K. and Finkel, R. C., The soil production function and landscape equilibrium. *Nature*, 1997, **388**, 358–361.
12. Valdiya, K. S., *Geology of Kumaun Lesser Himalaya*, Wadia Institute of Himalayan Geology, Dehradun, 1980, p. 228.
13. Ahmad, T., Harris, N., Bickle, M., Chapman, H., Bunbury, J. and Prince, C., Isotopic constraints on the structural relationships between the Lesser Himalayan Series and the High Himalayan Crystalline Series, Garwhal Himalaya. *Geol. Soc. Am. Bull.*, 2000, **112**, 467–477.
14. Islam, R. and Thakur, V. C., Geology of Bhilangna valley, Garhwal Himalaya. *Geosci. J.*, 1988, **9**(2), 143–152.
15. Islam, R., Purohit, K. K. and Thakur, V. C., The birth history of two granitic plutons of the Bhilangna valley of Garhwal Himalaya: a geochemical approach. *J. Geol. Soc. India*, 1991, **38**, 23–35.
16. Pal, S. K., *Geomorphology of River Terraces along Alaknanda Valley*, *Garhwal Himalaya*, B.R. Publishing Corporation, Delhi, 1986, p. 158.
17. Ahmad, T. and Tarney, J., Geochemistry and petrogenesis of Garhwal volcanics: implications for evolution of the north Indian lithosphere. *Precambrian Res.*, 1991, **50**, 69–88.
18. Stork, A. L., Smith, D. K. and Gill, J. B., Evaluation of geochemical reference standards by X-ray fluorescence analysis. *Geostand. Newslett.*, 1987, **11**, 107–113.
19. Saini, N. K., Mukherjee, P. K., Rathi, M. S. and Khanna, P. P., Evaluation of energy dispersive X-ray fluorescence spectrometry in the rapid analysis of silicate rocks using pressed powder pellets. *X-Ray Spectrometry*, 2000, **29**(2), 166–172.
20. Purohit, K. K., Saini, N. K. and Khanna, P. P., Geochemical dispersion pattern of heavy metal abundances in the intermontane Pinjaur Dun, Sub-Himalaya. *Himalayan Geol.*, 2010, **31**(1), 29–34.
21. Khanna, P. P., Saini, N. K., Mukherjee, P. K. and Purohit, K. K., An appraisal of ICP–MS technique for determination of REEs: long term QC assessment of silicate rock analysis. *Himalayan Geol.*, 2009, **30**(1), 95–99.
22. Nesbitt, H. W. and Young, G. M., Early Proterozoic climates and plate motions inferred from major element chemistry of lutites. *Nature*, 1982, **299**, 715–717.
23. Nesbitt, H. W. and Young, G. M., Prediction of some weathering trends of plutonic and volcanic rocks based on thermodynamic and kinetic considerations. *Geochim. Cosmochim. Acta*, 1984, **48**, 1523–1534.
24. Nesbitt, H. W. and Young, G. M., Formation and diagenesis of weathering profiles. *J. Geol.*, 1989, **97**, 129–147.
25. McLennan, S. M., Weathering and global denudation. *J. Geol.*, 1993, **101**, 295–303.
26. Condie, K. C., Chemical composition and evolution of the upper continental crust: contrasting results from surface samples and shales. *Chem. Geol.*, 1993, **104**, 1–37.
27. Nesbitt, H. W. and Wilson, R. E., Recent chemical weathering of basalts. *Am. J. Sci.*, 1992, **292**(10), 740–777.
28. Sun, S. S. and McDonough, W. F., Chemical and isotopic systematics of oceanic basalts: implications for mantle composition and processes. In *Magmatism in Ocean Basins* (eds Saunders, A. D. and Norry, M. J.), Geological Society Special Publication, 1989, vol. 42, pp. 313–345.
29. Aydin, D. N. S. and Aydin, A., Distribution of rare earth elements and oxyhydroxide phases within a weathered felsic igneous profile in Hong Kong. *J. Asian Earth Sci.*, 2009, **34**, 1–9.
30. Rainbird, R. H., Nesbitt, H. W. and Donaldson, J. A., Formation and diagenesis of a sub-Huronian saprolith: Comparison with a modern weathering profile. *J. Geol.*, 1990, **98**, 801–822.
31. Nedachi, Y., Nedachi, M., Bennett, G. and Ohmoto, H., Geochemistry and mineralogy of the 2.45 Ga Pronto paleosols, Ontario, Canada. *Chem. Geol.*, 2005, **214**, 21–44.
32. Harnois, L., The CIW index: A new chemical index of weathering. *Sediment. Geol.*, 1988, **55**, 319–322.
33. Fedo, C. M., Nesbitt, H. W. and Young, G. M., Unraveling the effects of potassium metasomatism in sedimentary rocks and paleosols, with implications for paleoweathering conditions and provenance. *Geology*, 1995, **23**, 921–924.

ACKNOWLEDGEMENTS. We thank Prof. A. K. Gupta, Director, WIHG for providing the necessary facilities to carry out this work. Drs. P. P. Khanna and N. K. Saini of WIHG are acknowledged for chemical analysis. Prof. Grant Young, University of Western Ontario is much appreciated for a lively discussion on CIA.

Received 3 October 2013; revised accepted 6 October 2014